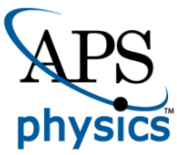

Electric-field-induced Majorana Fermions in Armchair Carbon Nanotubes

Jelena Klinovaja, Suhas Gangadharaiah, and Daniel Loss

Phys. Rev. Lett. **108**, 196804 — Published 8 May 2012

DOI: 10.1103/PhysRevLett.108.196804

Electric-Field Induced Majorana Fermions in Armchair Carbon Nanotubes

Jelena Klinovaja, Suhas Gangadharaiah, and Daniel Loss
Department of Physics, University of Basel, Klingelbergstrasse 82, 4056 Basel, Switzerland

We consider theoretically an armchair Carbon nanotube (CNT) in the presence of an electric field and in contact with an s-wave superconductor. We show that the proximity effect opens up superconducting gaps in the CNT of different strengths for the exterior and interior branches of the two Dirac points. For strong proximity induced superconductivity the interior gap can be of the p-wave type, while the exterior gap can be tuned by the electric field to be of the s-wave type. Such a setup supports a single Majorana bound state at each end of the CNT. In the case of a weak proximity induced superconductivity, the gaps in both branches are of the p-wave type. However, the temperature can be chosen in such a way that the smallest gap is effectively closed. Using renormalization group techniques we show that the Majorana bound states exist even after taking into account electron-electron interactions.

PACS numbers: 73.63.Fg, 74.45.+c

Introduction. Majorana fermions in solid state systems have attracted considerable attention recently [1–10]. In particular, the possibility of realizing them as bound states at the ends of semiconducting nanowires in the proximity of an s-wave bulk superconductor has led to much activity. Such setups require a Zeeman splitting, typically generated by an external magnetic field [11], that must be larger than the proximity induced gap to induce an effective p-wave superconductor in the topological phase. Such a magnetic field, however, tends to destroy the gap in the bulk superconductor itself, and thus a delicate balance must be found [12]. It is therefore very desirable to search for Majorana-scenarios which do not require magnetic fields.

One of the prerequisites for a Majorana bound end state (MBS) is the existence of helical modes, i.e. modes which carry opposite spins in opposite directions. It has been shown recently that such helical states are induced in Carbon nanotubes (CNT) via spin-orbit interaction (SOI) by an external *electric* field E [13, 14]. This mechanism works optimally for a special class of metallic CNTs: armchair CNTs (N, N). This class is characterized by a spin-degenerate low-energy spectrum around the two inequivalent Dirac points, K and K'. This degeneracy can be lifted by E which gives then rise to helical modes.

However, when putting the CNT in contact with an s-wave superconductor (see Fig. 1) with the goal to generate MBS the following problem is encountered. The two Dirac points K and K' are Kramers partners (see Fig. 2) and thus the superconducting pairing induced via the proximity effect will involve both of them, *i.e.* left (right)-moving electrons from the branch at K get paired with the right (left)-moving electrons from the branch at K' to form an s-wave Cooper pair with zero total momentum. This results in two superconducting gaps, an 'exterior' one, Δ_e, and an 'interior' one, Δ_i. Thus, in general, we expect *two* MBS at each end of the CNT (i.e. four in total). This, however, is problematic as the Majorana pair at a given end can combine to form a single fermion by local perturbations. Thus, the question then arises if there exists a regime with only one MBS at each end [15]. As we will show, the answer is affirmative but under rather stringent conditions. One of them requires a comparable tunnel coupling of the A and B sublattices of the CNT to the superconductor, see Fig. 1. Using the interference mechanism first described by Le Hur *et al.* [16], we will show that for this particular case Δ_e (Δ_i) gets enhanced (suppressed) due to constructive (destructive) interference in the tunneling process. If $\Delta_{e/i}$ is smaller (larger) than the gap opened by E, then the coupling between the two Dirac points is of p-wave type (s-wave type). This leads to two regimes for MBS. In the first one, only one of two branches has a p-wave gap, thus giving rise to only one MBS at each end of the CNT. In a second regime, where both branches have a potential for p-wave pairing, the temperature T can be chosen to lie between Δ_e and Δ_i, so that only the exterior branches will go fully superconducting, whereas the inte-

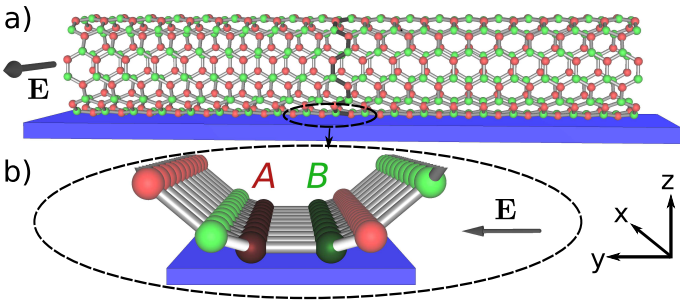

FIG. 1. (a) An armchair nanotube (cylinder) is placed on top of a superconductor (blue slab). The x-axis points along the nanotube. An electric field E is applied perpendicular to the nanotube, say along y-axis [17]. There are two non-equivalent lattice sites: A (light red) and B (light green). (b) The distances between the superconductor surface and the atoms of sublattice A (dark-red row) and of sublattice B (dark-green row) are assumed the same. Thus, the tunneling amplitudes to the different sublattices are (nearly) equal.

rior branches stay normal. Again, a single pair of MBS in the CNT emerges. We further investigate the effect of interactions on the MBS. This is particularly important for the second regime due to the presence of gapless states from the interior branches that could be harmful to the MBS. However, using bosonization techniques we will dispel these concerns and show that for screened interactions the MBS remain stable although they can get substantially delocalized similar to the simpler case of Rashba wires [8].

Nanotube spectrum. We consider an armchair CNT in the presence of an electric field E applied perpendicular to the CNT axis (see Fig. 1)[17]. Taking into account the spin-orbit interaction the low-energy sector is described by an effective Hamiltonian around the Dirac points given by [13]

$$\mathcal{H} = \hbar v_F k \tau_3 \sigma_2 + \tau_3 e E \xi S_z \sigma_2 + \alpha S_x \sigma_1, \qquad (1)$$

where k is the momentum along the nanotube axis taken from the Dirac point, σ_i is the Pauli matrix on the sublattice space (A, B) associated with the honeycomb unit cell, and S_i is the spin operator with eigenvalues ± 1. The Pauli matrix τ_i acts on the K, K'-subspace. Here, $v_F \simeq 10^6$ m/s is the Fermi velocity, and the parameter α arises from the interplay between SOI and curvature effects [13, 18, 19]. In the framework of the tight-binding model, $\alpha = -0.08\,\mathrm{meV}/R[\mathrm{nm}]$, where R is the radius of the CNT [13]. The parameter $\xi \simeq 2\times 10^{-5}$nm is given by a combination of hopping matrix elements, on-site dipole moment, and SOI [14].

The spectrum given by $\mathcal{H}$ (Eq. 1) consists of four branches (see Fig. 2), $\varepsilon_n(k) = \pm eE\xi \pm \sqrt{\alpha^2 + (\hbar v_F k)^2}$ for each Dirac point. In the following, we label the four branches by $n = 1, ..., 4$. For each k, $n = 1$ corresponds to the highest eigenvalue and $n = 4$ to the lowest. The remarkable feature of the spectrum is the existence of helical modes, which carry opposite spins in opposite directions. The average value of the spin along the CNT-axis ($\langle S_x \rangle$) or parallel to E-field ($\langle S_y \rangle$) is equal to zero. The projection of the spin along the z-direction is equal to $\langle S_z \rangle = \sin\zeta$, where ζ is defined by $\zeta = \arcsin(\hbar v_F k/\sqrt{\alpha^2 + (\hbar v_F k)^2})$ and depends on the wavevectror k. Note that the eigenvectors $\psi^{e/i}_{nK}$ and $\psi^{e/i}_{nK'}$ are independent of E. For a (10,10)-CNT and $E = 1$V/nm, and with a Fermi level μ tuned between the two lowest electronic states polarizations close to 90% can be reached [14].

Proximity induced superconductivity. If a CNT is in contact with an s-wave bulk superconductor, then the proximity effect induces superconductivity also in the CNT which at the BCS mean-field level is described by

$$\sum_{i,j,i',j',s} (\Delta_d c^\dagger_{ip_r s} c^\dagger_{jp_r \bar{s}} + \Delta_n c^\dagger_{i'p_r s} c^\dagger_{j'p_r \bar{s}}) + h.c., \qquad (2)$$

where we concentrate on the contribution coming from the π-bands formed by the radial p_r-orbitals [13, 20].

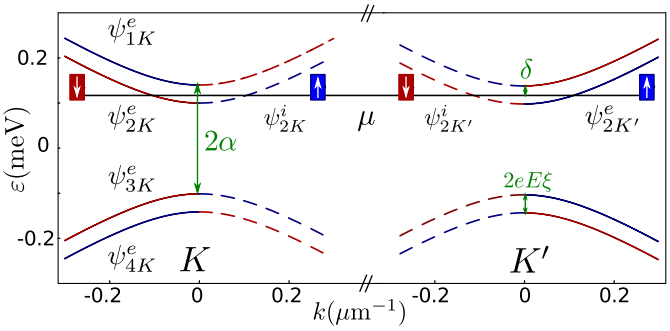

FIG. 2. The energy spectrum around the Dirac points K, K' for a (10,10)-CNT in an electric field $E = 1$ V/nm, which consists of exterior (full line) and interior (dashed line) branches. Each branch of the spectrum is characterized by the sign of the spin projection along the z-axis $\langle S_z \rangle$ (red: spin down, blue: spin up). The Fermi level μ lies inside the gap given by $2eE\xi$, and $\delta = eE\xi + \alpha - \mu$.

Here, $c^{(\dagger)}_{ip_r s}$ are the standard fermionic annihilation (creation) operators, with s and $\bar{s}$ denoting opposite spin states. The sum runs over atoms which are in contact with the bulk superconductor: i and j belong to the same sublattice, whereas i' and j' belong to different sublattices. Generically, the lattice constant of the superconducting material is not commensurate with the one of graphene. The CNT is placed in such a way that the distance from the superconducting surface to the A and B atoms is the same (see Fig. 1), which is satisfied for armchair CNTs. This ensures equal probability amplitude for tunneling to either sublattice. Since the phase of the superconducting order parameter $\Delta_{d/n}$ can be chosen arbitrary, we assume them to be real. The coupling terms in Eq. (2) conserve momentum, so they pair Kramers partners from the opposite Dirac cones. The process in which the Cooper pair tunnels from the superconductor to either one of the sublattice σ is written as

$$\Delta_d \sum_{\sigma,s,\kappa} \mathrm{sgn}(\sigma\bar{s}) \psi^\dagger_{\sigma s\kappa} \psi^\dagger_{\sigma\bar{s}\bar{\kappa}} + h.c.\,, \qquad (3)$$

where the indices κ and $\bar{\kappa}$ denote opposite Dirac points. The operators $\psi_{\sigma s\kappa}$ and $c_{ip_r s}$ are connected via Fourier transformation [14]. The pairing term between electrons in different sublattices are

$$i\Delta_n \sum_{\sigma,s,\kappa} \mathrm{sgn}(\bar{s}) \psi^\dagger_{\sigma s\kappa} \psi^\dagger_{\bar{\sigma}\,\bar{s}\bar{\kappa}} + h.c. \qquad (4)$$

To simplify the notation we introduce Pauli matrices η_i which act on the particle-hole subspace, and we work in the basis $\widetilde{\mathbf{\Psi}} = (\mathbf{\Psi}, \mathbf{\Psi}^\dagger)$, with $\mathbf{\Psi} = (\psi_{A\uparrow K}, \psi_{B\uparrow K}, \psi_{A\downarrow K}, \psi_{B\downarrow K}, \psi_{A\uparrow K'}, \psi_{B\uparrow K'}, \psi_{A\downarrow K'}, \psi_{B\downarrow K'})$. This allows us to rewrite Eqs. (3) and (4) in a compact form $H_{sc} = \widetilde{\mathbf{\Psi}}^\dagger \mathcal{H}_{sc} \widetilde{\mathbf{\Psi}}$,

$$\mathcal{H}_{sc} = -\eta_2 \tau_1 S_y \Delta_d\ \sigma_3 + \eta_1 \tau_1 S_y \Delta_n\ \sigma_1. \qquad (5)$$

In the same basis, $\mathcal{H}$ in Eq. (1) can be rewritten as $\mathcal{H} = \frac{1}{2}(\hbar v_F k\sigma_2 + eE\xi\eta_3\tau_3 S_z\sigma_2 + \alpha\eta_3 S_x\sigma_1)$. To express the coupling between the different energy states in a canonical form we work in the basis of eigenvectors $\{\psi^e_{nK}, \psi^i_{nK}, \psi^e_{nK'}, \psi^i_{nK'}\}$. For the states at the Fermi level, $n = 2$, H_{sc} becomes

$$\sum_{l=e,i} \Delta_l(\psi^l_{2K'}\psi^l_{2K} - \psi^l_{2K}\psi^l_{2K'}) + h.c.\,, \tag{6}$$

with different coupling strengths for the exterior (e) and interior (i) branches,

$$\Delta_{e/i} = \Delta_d \pm \Delta_n\,|\sin\zeta|\,. \tag{7}$$

We note that the sign reflects the constructive and destructive interference, *resp.*, in the tunneling process from the bulk-superconductor into the CNT [16]. The final effective Hamiltonian for states at the Fermi level (expressed in terms of right- and left-movers, see below) takes the form $\mathcal{H}_{n=2} = \mathcal{H}_e\beta_e + \mathcal{H}_i\beta_i$, where $\mathcal{H}_l = k\tau_3 - \Delta_l\eta_2\tau_2$, where $\beta_{e/i} = (1 \pm \beta_3)/2$ (with the Pauli matrix β_3) acts on the exterior/interior branch subspace. $\mathcal{H}_l$ describes a one-dimensional p-wave topological superconductor of class DIII, satisfying time reversal, particle-hole, and chirality symmetry [22]. In Eq. (6), we neglected a term $\Delta_n \cos\zeta$ characterizing the coupling between $\psi^{e/i}_{2K}$ and $\psi^{e/i}_{4K'}$ which are separated by the particle-hole gap 2α, see Fig. 2. In the following we consider the limit of equal diagonal and non-diagonal parameters, *i.e.*, $\Delta_d \approx \Delta_n$ [21]. We note that for $k \gg \alpha/\hbar v_F$ the coupling between the interior branches is close to zero and that between the exterior branches is equal to $2\Delta_d$. We show that this asymmetry in the coupling strengths is crucial for the existence of Majorana bound states in CNTs.

Majorana bound states. Next, we obtain the MBS following the derivation of Ref. [8]. For illustrative purposes we derive the bound states that arise by considering the exterior branches. The field corresponding to the exterior branch is defined as, $\psi_e(x) = \psi^R_{2K}(x)e^{i(k_F+K)x} + \psi^L_{2K'}(x)e^{-i(k_F+K)x}$, where $\psi^R_{2K}(x)$ and $\psi^L_{2K'}(x)$ are the slowly moving right and left components about the K and K' points, *resp.* Denoting the length of the CNT by L, the boundary conditions, $\psi_e(x = 0) = \psi_e(x = L) = 0$, yield the restriction $\psi^R_{2K}(x) = -\psi^L_{2K'}(-x)$. Thus, the kinetic term is given by $H^{(1)}_0 = -iv_F\int_{-L}^{L}\psi^{R\dagger}_{2K}(x)\partial_x\psi^R_{2K}(x)$, and the p-wave pairing term between the exterior branches by

$$-\Delta_e\int_{-L}^{L} dx\,\mathrm{sgn}(x)[\psi^R_{2K}(x)\psi^R_{2K}(-x) + h.c.]\,. \tag{8}$$

Solving for the zero energy mode localized around $x = 0$, we obtain the MBS $\Psi^M_e(x) \propto \gamma_e \sin[(K + k_F)x]e^{-x/\xi_e}$, where $\gamma_e = \gamma_e^\dagger$, and it is assumed that the localization length, given by $\xi_e = \hbar v_F/2\Delta_e$, satisfies $\xi_e \ll L$. Similarly for the interior branches, with the index e replaced by i.

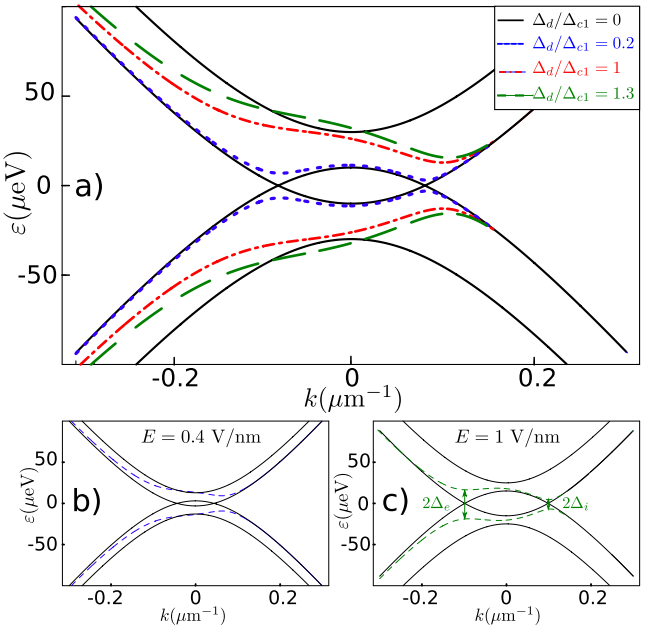

FIG. 3. The particle-hole spectrum of a CNT (10,10) in the presence of an electric field E with the Fermi level μ tuned inside the energy gap between the two upper branches (solid black lines). All energies are counted from $\mu = 0.11$ meV (see Fig. 2). By proximity effect, superconducting gaps $\Delta_{e,i}$ are opened at the Fermi points k_F. (a) Here, the E-field is fixed at 1 V/nm and Δ_d is varied. for $\Delta_d = 5\ \mu$eV $< \Delta_{c1}$ both branches are in the p-wave phase (dotted blue line). At the critical value $\Delta_d = 23\ \mu\text{eV} = \Delta_{c1}$ the gaps induced by the proximity effect and by E are equal (dot-dashed red line). For $\Delta_d = 30\ \mu\text{eV} > \Delta_{c1}$ only the interior branch is in the p-wave phase (dashed green line). Keeping Δ_d constant at 11 μeV and changing E, one goes from a regime [dashed blue line in (b)] with $E = 0.4$ V/nm $< \mathrm{E_{c1}} = 0.6$ V/nm where only the interior branch is in the p-wave phase to a regime [dashed green line (c)] with $E = 1$ V/nm $> \mathrm{E_{c1}} = 0.6$ V/nm where both branches are in the p-wave phase.

In general, the Majorana modes arising from the interior and exterior branches at the same end of the CNT are not protected and can combine into a fermion. To avoid such a scenario one needs to ensure the presence of only one single MBS at each end of the CNT. This can be achieved in two ways.

First, there is a window where the electric field E can be chosen in such a way that the superconductivity in the exterior branch can be tuned into a non-topological s-wave superconductor, while the interior one still remains a topological p-wave superconductor of class DIII [22] (see also above). In this case, only the interior branch supports a MBS at each end of the nanotube, and we refer to this as a topological phase of the CNT (see dashed green line in Fig. 3a). Concretely, such a regime is reached for $\Delta_e(k_F) > \delta > \Delta_i(k_F)$, where $k_F \approx \sqrt{(\mu + eE\xi)^2 - \alpha^2}/\hbar v_F$ and $\delta = eE\xi + \alpha - \mu$. With Eq. (7) this criterion becomes equivalent to $\Delta_{c2} \gtrsim \Delta_d \gtrsim$

Δ_{c1}, where $\Delta_{c1/c2} = \delta/(1 \pm \sin\zeta)$. For a given value of Δ_d, the experimentally viable approach to drive the system into the topological phase is to tune the electric field E. Indeed, for $E_{c1} \gtrsim E \gtrsim E_{c2}$ (see Fig. 3b) the exterior branch is in the s-wave phase, while the interior one is in the p-wave phase. The critical value of the electric field E_{c1} (E_{c2}) is determined by the condition $\delta = \Delta_e(k_F)$ ($\delta = \Delta_i(k_F)$) [23]. Similarly, we can tune between the phases by changing the Fermi level. [In passing we note that the gap $eE\xi$, and thus δ, get enhanced by interaction effects around $k = 0$ [24], which is useful for experimental realizations. However, for simplicity we will ignore this feature here.]

Second, in the regime $\Delta_d \lesssim \Delta_{c1}$ (see dotted blue line in Fig. 3a) or $E \gtrsim E_{c1}$ (see Fig. 3c) both branches are dominated by p-wave pairing. If the temperature is lower than both gaps, *i.e.* $k_BT < \Delta_{e,i}$, then there is an even number of MBS at each end of the nanotube, and the CNT is in the topologically trivial phase. However, in the intermediate regime with $\Delta_e > k_BT > \Delta_i$ [25], the interior gap Δ_i is closed and the Majorana states are removed, yet those from the exterior branches remain, and the CNT is again in the topological phase. In the following we consider this latter scenario and discuss the role of interactions coming from the gapless states of the interior branch.

Interactions. Interactions effects are most conveniently described by linearizing the spectrum of the fermionic fields $\psi^{e/i}_{2K}$ and $\psi^{e/i}_{2K'}$ near the Fermi momentum k_F and expressing them in terms of the bosonized fields. The quadratic part of the bosonized Hamiltonian thus obtained has the following form,

$$H_0 = \frac{1}{2}\sum_{n=\pm}\{\upsilon_n K_n(\partial_x\theta_n)^2 + \frac{\upsilon_n}{K_n}(\partial_x\phi_n)^2\}, \qquad (9)$$

where $\partial_x\phi_+$ and $\partial_x\phi_-$ are the sum and difference of densities between the two fermionic bands. The fields conjugate to them are defined as, θ_+ and θ_-, *resp.* The parameters $K_+ \simeq 1 - U_0/\pi\upsilon$ and $K_- \simeq 1 + (1 - \langle S_z\rangle^2)U_{2k_F}/2\pi\upsilon$ encode information about the interactions and the renormalized velocities are given as $\upsilon_+ \simeq \upsilon_F + U_0/\pi$, and $\upsilon_- \simeq \upsilon_F + b'(1 + \langle S_z\rangle^2)/4\pi$, where the b'-term [26, 27] is due to the backscattering contribution. Here, $U_{0,2k_F}$ denotes the Fourier component of the screened Coulomb interaction. Since $\langle S_z\rangle^2 < 1$ and thus $K_- > 1$, we conclude [28] that the forward scattering term $\propto \int dx d\tau \cos(\sqrt{8\pi}\phi_-)$ scales to zero.

Additional terms induced by the proximity effect lead to a modified Hamiltonian given by

$$H = H_0 + \frac{\Delta_e}{2\pi a}\cos\sqrt{2\pi}(\theta_+ - \phi_-). \qquad (10)$$

Since we assume here $\Delta_e > k_BT > \Delta_i$, the term due to the interior branches, $\frac{\Delta_i}{2\pi a}\cos\sqrt{2\pi}(\theta_+ + \phi_-)$, is smeared out by temperature effects and will not be considered.

Using standard techniques [28, 29], we derive the following renormalization group (RG) equations,

$$\frac{dK_+}{dl} = \frac{f^2}{4}\left(1 + \frac{4\gamma K_+K_-}{(1+\gamma)^2}\right), \qquad (11)$$

$$\frac{dK_-^{-1}}{dl} = \frac{f^2}{4}\left(1 + \frac{4\gamma}{K_-K_+(1+\gamma)^2}\right), \qquad (12)$$

$$\frac{d\gamma}{dl} = \frac{f^2}{4}\frac{\gamma(1-\gamma)K_+}{(1+\gamma)(K_+K_- + 1)}, \qquad (13)$$

$$\frac{df}{dl} = f\left(2 - \frac{1}{2K_+} - \frac{K_-}{2}\right), \qquad (14)$$

where the flow parameter $l = \ln[a/a_0]$, $f = 2\Delta_e a$, and γ is the ratio of the velocities υ_+/υ_-. We note that for the non-interacting case γ is already at its fixed point, $\gamma = 1$, and including interactions (the repulsive interactions are assumed to be well screened) causes only a small deviation from unity [30, 31]. Thus, it is convenient to assume $\gamma = 1$, and under this assumption K_+K_- is a constant, given in leading order by unity. Above RG equations now acquire the simple form $dR/dl = f^2/2$ and $df/dl = f(2 - 1/R)$, where $R = (1/K_+ + K_-)/2$. These equations are exactly the same as in Ref. [8] derived for interacting spinless fermions in an effective p-wave regime. We conclude that for a CNT whose initial values of the parameters lie in the regime $f_0 > 2\sqrt{2R_0 - \ln(2R_0 e)}$ has its RG flow such that both K_+ and K_- approach the non-interacting value. At this point the problem can be refermionized into a set of decoupled gapped and gapless fermions and for a strongly screened CNT with initial value *e.g.* $K_+ = 0.8$ the localization length ξ_e increases by 25%. Therefore, we conclude that the MBS which arise from gapped fermions remain protected even in the presence of interacting gapless fermions and simply acquire a renormalized ξ_e.

Conclusions. We have shown that an armchair CNT with helical modes generated by an external electric field is a promising candidate material for Majorana bound states. By placing the CNT on top of an s-wave superconductor and tuning the Fermi level and the electric field, one can induce pairing of Kramers partners from opposite Dirac points. This pairing opens up inequivalent gaps for the exterior and the interior branches. The Majorana modes obtained are stabilized by either tuning the electric field such that the exterior gap acquires a predominantly s-wave character or by increasing the temperature to remove the pairing in the interior branches.

Acknowledgements. We thank Karsten Flensberg for valuable discussions in the initial stage of this work. We also acknowledge helpful discussions with Diego Rainis and Pascal Simon. This work is supported by the Swiss NSF, NCCR Nanoscience and NCCR QSIT, and DARPA.

[1] L. Fu and C. L. Kane, Phys. Rev. Lett. **100**, 096407 (2008).

[2] A. R. Akhmerov, J. Nilsson, and C. W. J. Beenakker Phys. Rev. Lett. **102**, 216404 (2009).

[3] R. M. Lutchyn, J. D. Sau, and S. Das Sarma, Phys. Rev. Lett. **105**, 077001 (2010).

[4] Y. Oreg, G. Refael, and F. von Oppen, Phys. Rev. Lett. **105**, 177002 (2010).

[5] A. C. Potter and P. A. Lee, Phys. Rev. B **83**, 094525 (2011).

[6] J. Alicea, Phys. Rev. B **81**, 125318 (2010).

[7] X. L. Qi and S. C. Zhang, Rev. Mod. Phys. **83**, 1057 (2011).

[8] S. Gangadharaiah, B. Braunecker, P. Simon, and D. Loss, Phys. Rev. Lett. **107**, 036801 (2011).

[9] E. M. Stoudenmire, J. Alicea, O. Starykh, and M.P.A. Fisher, Phys. Rev. B **84**, 014503 (2011).

[10] R. M. Lutchyn and M.P.A. Fisher, arXiv:1104.2358.

[11] The Zeeman splitting can also be generated internally e.g. by the Overhauser field coming from the hyperfine interaction between nuclear and electron spins [32].

[12] T. D. Stanescu, R. M. Lutchyn, and S. Das Sarma, Phys. Rev. B **84**, 144522 (2011).

[13] J. Klinovaja, M. J. Schmidt, B. Braunecker, and D. Loss, Phys. Rev. Lett. **106**, 156809 (2011).

[14] J. Klinovaja, M. J. Schmidt, B. Braunecker, and D. Loss, Phys. Rev. B **84**, 085452 (2011).

[15] A recent proposal for MBS in CNTs focuses on the spectrum around the Γ-point [33] (instead of the K, K'-points with a Dirac spectrum considered here), where this difficulty would be absent in principle. However, the effective Hamiltonian around the Γ-point for a realistic CNT with SOI is not known and needs separate treatment.

[16] K. Le Hur, S. Vishveshwara, and C. Bena, Phys. Rev. B **77**, 041406 (2008).

[17] We note that all E-field directions in the yz-plane of Fig. 1 are equivalent. Also, by placing metal gates on top and bottom of the CNT, the electric field and the chemical potential can be tuned independently.

[18] W. Izumida, K. Sato, and R. Saito, J. Phys. Soc. Jpn. **78**, 074707 (2009).

[19] J.-S. Jeong and H.-W. Lee, Phys. Rev. B **80**, 075409 (2009).

[20] R. Saito, G. Dresselhaus, and M. S. Dresselhaus, *Physical Properties of Carbon Nanotubes* (Imperial College Press, London, 1998).

[21] The induced superconductivity matrix elements depend on the probability for the electrons to tunnel on either the A or the B site, which due to the symmetry of the problem (see Fig. 1) should be similar. A small difference between Δ_d and Δ_n (Δ_e and Δ_i are still considerably different) would not change our main results.

[22] S. Ryu, A. P. Schnyder, A. Furusaki, and A. W. W. Ludwig, New Journal of Physics **12**, 065010 (2010).

[23] See Supplemental Material at http://link.aps.org/ supplemental/XYZ/PhysRevLett.XXX for a plot of the phase diagram.

[24] B. Braunecker, G. I. Japaridze, J. Klinovaja, and D. Loss, Phys. Rev. B **82**, 045127 (2010).

[25] For $\Delta_d \sim 5$ μeV, we require 10mK $<$ T $<$ 100mK.

[26] R. Egger and A. Gogolin, Phys. Rev. Lett. **79**, 5082 (1997); Eur. Phys. J. B **3**, 23 (1998).

[27] C. Kane, L. Balents, and M.P.A. Fisher, Phys. Rev. Lett. **79**, 5086 (1997).

[28] T. Giamarchi, *Quantum Physics in One Dimension*, (Clarendon Press, Oxford, 2004).

[29] A. O. Gogolin, A. A. Nersesyan, and A. M. Tsvelik, *Bosonization and Strongly Correlated Systems*, (University Press, Cambridge, 1998).

[30] O. A. Starykh, D. L. Maslov, W. Haeusler, and L. I. Glazman, in Lecture Notes in Physics, ed. T. Brandes, vol. 544, p.37, 1999.

[31] J. Klinovaja, S. Gangadharaiah, and D. Loss, in preparation.

[32] B. Braunecker, P. Simon, and D. Loss, Phys. Rev. B **80**, 165119 (2009).

[33] J. D. Sau and S. Tewari, arXiv:1111.5622.